New Perspective on the Formation and Reactivity of Metal−Metal-Bonded Dinuclear Rhodium and Iridium Complexes

Cristina Tejel, Miguel A. Ciriano,* José A. López, Fernando J. Lahoz, and Luis A. Oro*

Departamento de Química Inorgánica, Instituto de Ciencia de Materiales de Aragón, Universidad de Zaragoza-CSIC, E-50009 Zaragoza, Spain

Received April 23, 1997[⊗]

Reactions of the binuclear complexes [{M(μ-Pz)(CNBu^t)$_2$}$_2$] (M = Rh (**1**), Ir (**2**); Pz = pyrazolate) with diiodine give the metal−metal-bonded complexes [{M(μ-Pz)(I)(CNBu^t)$_2$}$_2$] (M = Rh (**3**), Ir (**4**)). A further reaction with diiodine afford the complexes [{M(μ-Pz)(I)(CNBu^t)$_2$}$_2$(μ-I)]I, which react cleanly with CF_3SO_3Me replacing the ionic iodide by the triflate group. The M(I) complexes **1** and **2** are easily oxidized by mild oxidants such as $[Cp_2Fe]^+$ to give the metal−metal-bonded dications [{M(μ-Pz)(CNBu^t)$_2$(MeCN)}$_2$]$^{2+}$, which add halide ions yielding the neutral complexes [{M(μ-Pz)(X)(CNBu^t)$_2$}$_2$] (M = Rh, X = Cl (**7**); M = Rh, Ir, X = I). These reactions indicate that the metal−metal bond formation has an electron-transfer character. Evidence of the nucleophilic attack by the metal−metal bond in complexes **3** and **4** of small molecules such as diiodine is provided by the reaction of $[I(Py)_2]BF_4$ with **7**, which adds the electrophilic iodine(I) to give the bridging iodide complex [{Rh(μ-Pz)(Cl)(CNBu^t)$_2$}$_2$(μ-I)]$^+$. In addition, an electrophile such as $MeCF_3SO_3$ abstracts one of the iodide ligands *trans* to the metal−metal bond in **3** to give MeI and the cationic complex [Rh$_2$(μ-Pz)$_2$(I)(CNBu^t)$_4$]CF_3SO_3. This cation adds complex **3**, which behaves as a metalloligand through an iodide atom, to give the tetranuclear complex [{Rh$_2$(μ-Pz)$_2$(I)(CNBu^t)$_4$}$_2$(μ-I)]CF_3SO_3 (**8**). The X-ray structure of **8** contains two metal−metal-bonded binuclear 'Rh$_2$(μ-Pz)$_2$(I)(CNBu^t)$_4$' units linked through a slightly asymmetric bridging iodine atom, showing an unusual Rh−I−Rh bond angle of 129.99(4)°. Reaction of **3** with IC≡C−Ph gives the acetylide complex [(CNBu^t)$_2$(I)Rh(μ-Pz)$_2$(μ-I)Rh(η^1-C≡C−Ph)(CNBu^t)$_2$]I. EHMO calculations on complexes [Rh$_2$(μ-Pz)$_2$(CNBu^t)$_4$]$^{2+}$, [Rh$_2$(μ-Pz)$_2$(I)(CNBu^t)$_4$]$^+$ [**A**]$^+$, and [{Rh(μ-Pz)(I)(CNBu^t)$_2$}$_2$] successfully explain the reactivity at the metal−metal bond, that of the iodide ligand in **3** with electrophiles, and those of [**A**]$^+$ with nucleophiles. Complex **3** and the cation [Rh$_2$(μ-Pz)$_2$(I)(CNBu^t)$_4$]$^+$ react with MeI in the presence of direct sunlight to give the oxidative-addition product [(CNBu^t)$_2$(I)Rh(μ-Pz)$_2$(μ-I)Rh(Me)(CNBu^t)$_2$]$^+$ in high yield.

Introduction

Recent studies on binuclear complexes of rhodium and iridium containing alkyl isocyanide ligands have shown a high electronic density at the metal centers[1] and may be considered to be "supernucleophiles"[2] due to their high reactivity. Thus, the complex [{Rh(μ-Pz)(CNBu^t)$_2$}$_2$] adds a variety of chlorocarbons with C−Cl bond cleavage to give dirhodium(III) complexes.[3,4] In particular, we recently reported[5] that the addition of methyl iodide to the binuclear complexes [{M(μ-L)(CNBu^t)$_2$}$_2$] and [(cod)M(μ-Pz)$_2$M(CNBu^t)$_2$] (M = Rh, Ir; L = pyrazolate (Pz), SBu^t) take place sequentially in two separate steps, each one at a single metal center for rhodium. These fast reactions lead to the M(III)−M(III) complexes even for iridium.

In contrast, metal−metal-bonded species generally result from oxidative-addition reactions to related binuclear iridium complexes. Thus, addition of MeI or I_2 to the complexes [{Ir(μ-L)(CO)(L′)}$_2$] (L = SBu^t,[6] pyrazolate,[7] 7-azaindolate,[8] 1,8-diamidonaphthalene;[9] L′ = monodentate phosphine or CO) and [{Ir(μ-Pz)(μ-SBu^t)(CO)(L′)}$_2$][10] in all cases resulted in the formation of the Ir(II)−Ir(II) species. Meanwhile, for rhodium, acetyl Rh(I)−Rh(III) complexes result[11] from the addition of MeI to [{Rh(μ-SBu^t)(CO)(L′)}$_2$], but Rh(II)−Rh(II) complexes result from the reaction of [{Rh(μ-L)(CO)(L′)}$_2$]

[⊗] Abstract published in *Advance ACS Abstracts,* September 15, 1997.

(1) Tejel, C.; Villoro, J. M.; Ciriano, M. A.; López, J. A.; Eguizábal, E.; Lahoz, F. J.; Bakhmutov, V. I.; Oro, L. A. *Organometallics* **1996**, *15*, 2967.

(2) Collman, J. P.; Brauman, J. I.; Madonik, A. M. *Organometallics* **1986**, *5*, 310.

(3) Ciriano, M. A.; Tena, M. A.; Oro, L. A. *J. Chem. Soc., Dalton Trans.* **1992**, 2123.

(4) Tejel, C.; Ciriano, M. A.; Oro, L. A.; Tiripicchio, A.; Ugozzoli, F. *Organometallics* **1994**, *13*, 4153.

(5) Tejel, C.; Ciriano, M. A.; Edwards, A. J.; Lahoz, F. J.; Oro, L. A. *Organometallics* **1997**, *16*, 45.

(6) (a) El Amane, M.; Maisonnat, A.; Dahan, F.; Poilblanc, R. *New J. Chem.* **1988**, *12*, 661. (b) Kalck, P.; Bonnet, J.-J. *Organometallics* **1982**, *1*, 1211.

(7) (a) Bushnell, G. W.; Fjeldsted, D. O. K.; Stobart, S. R.; Wang, J. J. *Organometallics* **1996**, *15*, 3785. (b) Coleman, A. W. T.; Eadie, D. T.; Stobart, S. R. *J. Am. Chem. Soc.* **1982**, *104*, 922. (c) Beveridge, K. A.; Bushnell, G. W.; Dixon, K. R.; Eadie, D. T.; Stobart, S. R. *J. Am. Chem. Soc.* **1982**, *104*, 920. (d) Powell, J.; Kuksis, A.; Nyburg, S. C.; Ng, W. W. *Inorg. Chim. Acta* **1982**, *64*, L211.

(8) Ciriano, M. A.; Pérez-Torrente, J. J.; Oro, L. A. *J. Organomet. Chem.* **1993**, *445*, 273.

(9) Fernández, M. J.; Modrego, J.; Lahoz, F. J.; López, J. A.; Oro, L. A. *J. Chem. Soc., Dalton Trans.* **1990**, 2587.

(10) (a) Pinillos, M. T.; Elduque, A.; López, J. A.; Lahoz, F. J.; Oro, L. A. *J. Chem. Soc., Dalton Trans.* **1991**, 1391. (b) Pinillos, M. T.; Elduque, A.; Oro, L. A.; Lahoz, F. J.; Bonati, F.; Tiripicchio, A.; Tiripicchio-Camellini, M. *J. Chem. Soc., Dalton Trans.* **1990**, 989.

(11) Mayanza, A.; Bonnet, J.-J.; Galy, J.; Kalk, P.; Poilblanc, R. *J. Chem. Res., Synop.* **1980**, 146, *J. Chem. Res., Miniprint* **1980**, 2101.

S0276-7333(97)00347-6 CCC: $14.00

(L = 1,8-diamidonaphthalene) with diiodine.[12] The formation of a metal−metal bond in these reactions has been associated to the nature of the metal (favored for the transition metals in the third-row versus those in the second-row) and to the flexibility of the framework of metals and bridging ligands.[13,14] Noticeably, further breaking of the metal−metal bond is unusual, although it has been reported for some iridium complexes with SBu^t.[6b,10b]

We now present our reactivity studies of the binuclear supernucleophiles $[\{M(\mu\text{-Pz})(CNBu^t)_2\}_2]$ (M = Rh, Ir) with diiodine that, in contrast to our previous findings with methyl iodide, show the formation of metal−metal-bonded species $[\{M(\mu\text{-Pz})(I)(CNBu^t)_2\}_2]$. These complexes also result from electron-transfer reactions. We also report reactions of the new complexes with electrophiles occurring at the metal−metal bond and at the ligands *trans* to this bond. The former result in additions, and the latter result in an iodide abstraction to render a metal−metal-bonded cationic complex, which is able to add nucleophiles such as $[\{M(\mu\text{-Pz})(I)(CNBu^t)_2\}_2]$ to give an interesting coupled tetrarhodium cation.

Results and Discussion

Oxidative-Addition and Oxidation Reactions Leading to Metal−Metal Bond Formation. The binuclear complexes $[\{M(\mu\text{-Pz})(CNBu^t)_2\}_2]$ (M = Rh (**1**), Ir (**2**)) react with 1 molar equiv of diiodine to give the complexes $[\{M(\mu\text{-Pz})(I)(CNBu^t)_2\}_2]$ (M = Rh (**3**), Ir (**4**)), which are isolated as air-stable orange and yellow solids, respectively. The elemental analysis indicates the addition of only 1 mol of diiodine, and the ^1H and $^{13}C\{^1H\}$ NMR spectra are consistent with the presence of a single isomer of C_{2v} symmetry. Therefore, complexes **3** and **4** are formulated as the M(II)−M(II) (d^7−d^7) binuclear derivatives, where its diamagnetism indicates the spin-pairing via metal−metal bond formation and the iodo ligands are *trans* to the metal−metal bond. According to the oxidation of both metal centers, the two observed ν(CN) frequencies are *ca.* 87 cm^{-1} higher than in the starting M(I) compounds.

The reactions leading to **3** and **4** could be considered a two-electron transfer (ET) process giving the cation $[\{M(\mu\text{-Pz})(CNBu^t)_2\}_2]^{2+}$ followed by the incorporation of the iodide ligands. As no kinetic measurements are available, since the reactions are very fast, we have studied the proposed redox process and the subsequent incorporation of the iodide ligands separately.

Chemical Oxidations Leading to Metal−Metal Bond Formation. Addition of a mild oxidant such as $[Cp_2Fe]PF_6$ to a solution of **1** in acetonitrile gives the yellow complex $[\{Rh(\mu\text{-Pz})(CNBu^t)_2(CH_3CN)\}_2](PF_6)_2$ ($[\mathbf{5}](PF_6)_2$) in high yield. Solutions of $[\mathbf{5}](PF_6)_2$ in acetone or acetonitrile show molar conductivity values typical for a 2:1 electrolyte. The acetonitrile ligands are quite labile in solution. Broad signals for the pyrazolate ligands are observed in the ^1H NMR spectrum at room temperature due to the rapid exchange on the NMR time scale of acetonitrile with the acetone-d_6 solvent.

Scheme 1

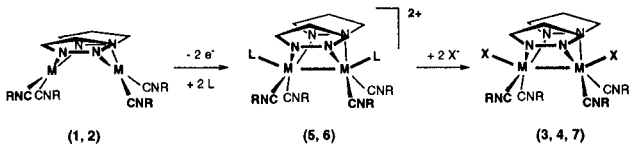

When the sample is cooled at 213 K, the ^1H NMR spectrum shows the presence of two complexes in a 6:4 ratio along with free acetonitrile. Comparison of the intensities of the coordinated acetonitrile (δ 2.75) and that of pyrazolate (δ 7.71) along with the C_{2v} symmetry of the major compound allows its identification as $[\{Rh(\mu\text{-Pz})(CNBu^t)_2(MeCN)\}_2]^{2+}$, while the C_s symmetry for the minor compound indicates the formula $[\{Rh(\mu\text{-Pz})(CNBu^t)_2\}_2(MeCN)(Me_2CO)]^{2+}$.

Oxidation of the iridium complex **2** with $[Cp_2Fe]PF_6$ in acetonitrile also occurs readily to give the white complex $[\{Ir(\mu\text{-Pz})(CNBu^t)_2(CH_3CN)\}_2](PF_6)_2$ ($[\mathbf{6}](PF_6)_2$) in quantitative yield. Characterization of $[\mathbf{6}](PF_6)_2$ relies on analytical and spectroscopic data, as commented for $[\mathbf{5}](PF_6)_2$. The acetonitrile ligands are more tightly bound for the iridium complex than for the rhodium counterpart, and thus, $[\mathbf{6}]^{2+}$ is the main compound in solution along with small amounts of the monosubstituted complex $[\{Ir(\mu\text{-Pz})(CNBu^t)_2\}_2(CH_3CN)(Me_2CO)]^{2+}$. Complexes $[\mathbf{5}]^{2+}$ and $[\mathbf{6}]^{2+}$ are, thus, Rh(II)−Rh(II) and Ir(II)−Ir(II) species, respectively, containing a metal−metal bond with labile ligands in a *trans* arrangement (Scheme 1).

Cyclic voltammetry experiments on the more stable complex **1** in acetonitrile, using NBu_4PF_6 as supporting electrolyte, show the presence of one fully irreversible oxidation peak at 201 mV (*vs* SCE). This is a two-electron process since the oxidation of **1** and **2** requires 2 molar equiv of $[Cp_2Fe]PF_6$ for the reactions to go to completion. The irreversibility in our case could be attributed to the coordination of acetonitrile to the oxidized species, $[\{Rh(\mu\text{-Pz})(CNBu^t)_2\}_2]^{2+}$, which prevents the regeneration of **1**.

Treatment of acetone-d_6 solutions of complexes **5** and **6** with a solution of KI results in the immediate displacement of the labile ligands and formation of complexes **3** and **4** quantitatively (^1H NMR evidence). Not surprisingly, addition of LiCl to a solution of **5** in acetone-d_6 gives the previously reported[3] complex $[\{Rh(\mu\text{-Pz})(Cl)(CNBu^t)_2\}_2]$ (**7**). The separation of the oxidative addition of iodine to **1** and **2** in two fomal steps, the chemical oxidation and the capture of the halide ligands, clearly indicates that the formation of the metal−metal bond has the nature of an electron-transfer (ET) reaction.

Interpretation of the Differences in the Oxidative-Addition Reactions of MeI and Diiodine. To form the homovalent M(II)−M(II) complexes, the two electrons should be removed from the HOMO, and in this way the metals act in a cooperative way, while the oxidation of a single metal center would lead to the mixed-valence M(I)−M(III) complexes. At this point, what produces the different type of behavior shown by the reactions of the $[\{M(\mu\text{-Pz})(CNBu^t)_2\}_2]$ (M = Rh, Ir) systems with MeI and with diiodine? The difference in the type of products should be attributed to the distinctive types of reaction, which is determined by the characteristics of the substrates. Thus, MeI has one

(12) Oro, L. A.; Fernández, M. J.; Modrego, J.; Foces-Foces, C.; Cano, F. H. *Angew. Chem., Int. Ed. Engl.* **1984,** *23*, 913.
(13) Fackler, J. P., Jr. *Polyhedron* **1997**, *16*, 1.
(14) He, X.; Maisonnat, A.; Dahan, F.; Poilblanc, R. *Organometallics* **1991**, *10*, 2443.

Scheme 2

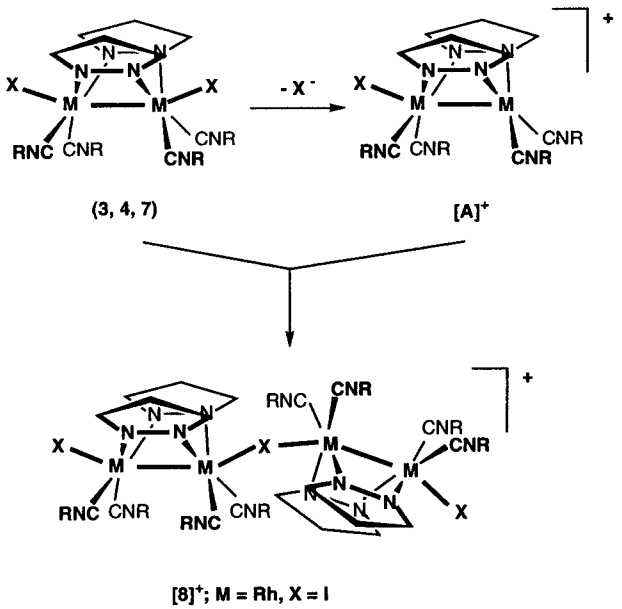

polarized I−C bond favorable for nucleophilic substitution by electron-rich metal centers, while diiodine is an oxidizing agent. The addition to a single metal center, as shown by the reactions with MeI, is favorable for supernucleophilic metal centers because it is a Lewis acid−base reaction in our case. On the contrary, the reactions with diiodine, leading to the metal−metal bond, involve a net electron transfer. This explanation could also be appropriated for the [{Ir(μ-NHR)(CO)$_2$}$_2$] complex, which also shows a different behavior toward MeI and diiodine.[15]

Abstraction of an Iodide Ligand *trans* to the Metal−Metal Bond. Formation and Structure of a Tetranuclear Complex. Complex **3** reacts quickly with 1 molar equiv of $MeCF_3SO_3$ in acetone to give MeI and a dark-red solution of the cationic complex [Rh$_2$(μ-Pz)$_2$(I)(CNBu^t)$_4$]CF_3SO_3 ([**A**]CF_3SO_3) (Scheme 2). Our initial attempts to isolate this complex only resulted in oils. However, the cation can be "trapped" as the adduct of [**A**]$^+$ with **3** linked through an iodide ligand. Thus, reaction of **3** with 0.5 molar equiv of $MeCF_3SO_3$ gives dichroic red-green monocrystals of [{Rh$_2$(μ-Pz)$_2$(I)(CNBu^t)$_4$}$_2$(μ-I)]CF_3SO_3 ([**8**]CF_3SO_3) in good yield. The analytical data of [**8**]CF_3SO_3 are in accordance with the proposed formula, and a definitive confirmation of its structure is obtained from an X-ray diffraction study.

Abstraction of the iodide ligand *trans* to the metal−metal bond by the cation Me$^+$ (as $MeCF_3SO_3$) is a method to create vacant coordination sites at this position, which can be covered by nucleophiles at this exo site of the complex. One of these nucleophiles is complex **3**. However, there are two sites in the binuclear complex **3** susceptible for an electrophilic attack, i.e., the metal−metal bond and the iodide ligands. The preference for the exo site by the Me$^+$ cation (as $MeCF_3SO_3$) should be attributed to the polar Rh−I bond, which facilitates the reaction, and to the difficulty of the methyl group to enter the endo site bridging the metal atoms.

The crystal structure of [**8**]CF_3SO_3 consists of tetranuclear rhodium(II) cations and triflate anions at

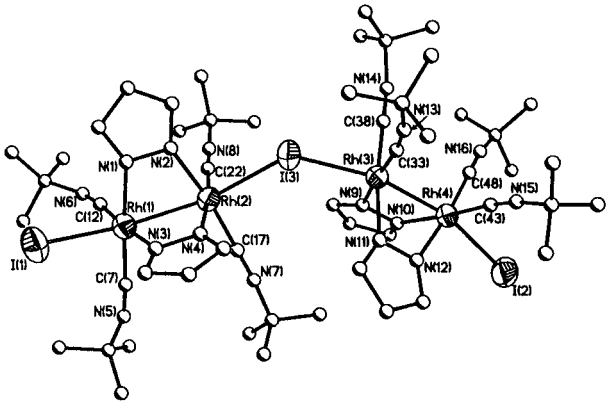

Figure 1. Molecular representation of the cation [{Rh$_2$(μ-Pz)$_2$(I)(CNBu^t)$_4$}$_2$(μ-I)]CF_3SO_3, [**8**]$^+$, with the numbering scheme used. Some carbon atoms are unlabeled for clarity.

normal van der Waals distances. The molecular structure of the tetranuclear cation [**8**]$^+$ (Figure 1) contains two binuclear "Rh$_2$(μ-Pz)$_2$(I)(CNBu^t)$_4$" units linked through a slightly asymmetric bridging iodine atom. Within each binuclear moiety the two metals exhibit a clear Rh−Rh bond doubly bridged by two bidentate pyrazolate ligands. Each metal completes a distorted octahedral environment with two terminal CNBu^t groups and two iodide atoms (one terminal and one bridging) located nearly opposite to the metal−metal bond (Rh−Rh−I$_{term}$ *av.* 163.51(3)°; Rh−Rh−I$_{bridg}$ *av.* 162.03(3)°). Although chemically equivalent, the two binuclear moieties Rh$_2$(μ-Pz)$_2$(I)(CNBu^t)$_4$ exhibit statistically different geometrical parameters, with the most evident distinctions affecting to the Rh−I and Rh−Rh bond distances (see Table 1).

The two Rh_2N_4 metallacycles adopt strongly puckered boat conformations (*av.* Q = 1.536(5) Å; θ = 89.9(3)°, ϕ = 0.0(3)°),[16] allowing short Rh−Rh separations. These intermetallic distances, 2.6320 and 2.6057(10) Å, compare well with those observed in other related Rh(II)−Rh(II) pyrazolate-bridged complexes with postulated Rh−Rh single bonds, such as [Rh(η^5-C$_5$H$_5$)(μ-Pz)]$_2$ (2.657(3) Å),[17] [Rh$_2$(μ-Pz)$_2$(I)$_2$(CO)$_2$(μ-dppm)] (2.612(3) Å),[18] and [Rh$_2$(μ-Pz)$_2$(μ-pc)(Br)(CO)(pcBr)] (2.581(1) Å) (pcBr = P(*o*-BrC$_6$F$_4$)Ph$_2$).[19] Besides these comparative values, the formation of the intermetallic bond is clearly corroborated by the large shortening of the intermetallic distance (1.28 Å; from 3.8996(6) Å in [{Rh(μ-Pz)(CNBu^t)$_2$}$_2$] to 2.6189(7) Å) upon the oxidative-addition reaction, by no means attributable to ligand steric requirements. Although other related binuclear pyrazolato-bridged rhodium complexes have also shown the exceptional flexibility of the Rh(μ-Pz)Rh framework,[10b] our example displays, as far as we know, the greatest change in the intermetallic separation upon the formation of the metal−metal bond.

As expected, the bridging Rh−I distances, 2.7900(10) and 2.8124(10) Å, are significantly longer than those of the terminal iodide ligands, 2.7545(10) and 2.7279(10) Å. The latter ones are similar to those reported for the complexes [Rh$_2$(μ-Pz)(I)$_2$(CNBu^t)$_2$(μ-dppm)$_2$]$^+$ (2.738(3)

(15) Kolel-Veetil, M. K.; Rheingold, A. L.; Ahmed, K. J. *Organometallics* **1993**, *12*, 3439.

(16) Cremer, D.; Pople, J. A. *J. Am. Chem. Soc.* **1975**, *97*, 1354.

(17) Bailey, J. A.; Grundy, S. L.; Stobart, S. R. *Organometallics* **1990**, *9*, 536.

(18) Oro, L. A.; Pinillos, M. T.; Tiripicchio, A.; Tiripicchio-Camellini, M. *Inorg. Chim. Acta* **1985**, *99*, L13.

(19) Barceló, F.; Lahuerta, P.; Ubeda, M. A.; Foces-Foces, C.; Cano, F. H.; Martínez-Ripoll, M. *J. Chem. Soc., Chem. Commun.* **1985**, 43.

Table 1. Selected Bond Lengths (Å) and Angles (deg) for the Cation [8]$^+$ [a]

Rh(1)−Rh(2)	2.6320(10)	Rh(3)−Rh(4)	2.6057(10)
Rh(1)−I(1)	2.7545(10)	Rh(4)−I(2)	2.7279(10)
Rh(2)−I(3)	2.7900(10)	Rh(3)−I(3)	2.8124(10)
Rh(1)−N(1)	2.042(8)	Rh(4)−N(10)	2.061(8)
Rh(2)−N(2)	2.031(7)	Rh(3)−N(9)	2.038(8)
Rh(1)−N(3)	2.038(8)	Rh(4)−N(12)	2.028(7)
Rh(2)−N(4)	2.051(8)	Rh(3)−N(11)	2.031(8)
Rh(1)−C(7)	1.958(12)	Rh(4)−C(43)	1.927(10)
Rh(1)−C(12)	1.896(11)	Rh(4)−C(48)	1.949(11)
Rh(2)−C(17)	1.929(11)	Rh(3)−C(33)	1.910(12)
Rh(2)−C(22)	1.935(11)	Rh(3)−C(38)	1.898(11)
Rh(2)−Rh(1)−I(1)	161.31(4)	Rh(3)−Rh(4)−I(2)	165.71(4)
Rh(2)−Rh(1)−N(1)	71.6(2)	Rh(3)−Rh(4)−N(10)	71.9(3)
Rh(2)−Rh(1)−N(3)	71.3(2)	Rh(3)−Rh(4)−N(12)	72.1(2)
Rh(2)−Rh(1)−C(12)	105.1(3)	Rh(3)−Rh(4)−C(43)	100.1(3)
Rh(2)−Rh(1)−C(7)	104.6(3)	Rh(3)−Rh(4)−C(48)	102.9(3)
I(1)−Rh(1)−N(1)	95.4(2)	I(2)−Rh(4)−N(10)	100.5(3)
I(1)−Rh(1)−N(3)	95.4(2)	I(2)−Rh(4)−N(12)	95.9(2)
I(1)−Rh(1)−C(7)	89.1(3)	I(2)−Rh(4)−C(43)	87.0(3)
I(1)−Rh(1)−C(12)	87.7(3)	I(2)−Rh(4)−C(48)	88.5(3)
N(1)−Rh(1)−N(3)	87.5(3)	N(10)−Rh(4)−N(12)	88.0(3)
N(1)−Rh(1)−C(7)	174.9(4)	N(10)−Rh(4)−C(43)	171.9(4)
N(1)−Rh(1)−C(12)	89.8(4)	N(10)−Rh(4)−C(48)	87.6(4)
N(12)−Rh(4)−C(43)	88.1(3)	N(3)−Rh(1)−C(12)	176.1(4)
N(12)−Rh(4)−C(48)	174.2(4)	N(3)−Rh(1)−C(7)	94.5(4)
C(7)−Rh(1)−C(12)	88.0(5)	C(43)−Rh(4)−C(48)	95.7(4)
Rh(1)−Rh(2)−I(3)	158.16(4)	Rh(4)−Rh(3)−I(3)	165.89(4)
Rh(1)−Rh(2)−N(2)	71.4(2)	Rh(4)−Rh(3)−N(9)	71.7(2)
Rh(1)−Rh(2)−N(4)	71.7(2)	Rh(4)−Rh(3)−N(11)	71.9(2)
Rh(1)−Rh(2)−C(17)	101.5(3)	Rh(4)−Rh(3)−C(33)	104.2(3)
Rh(1)−Rh(2)−C(22)	100.7(3)	Rh(4)−Rh(3)−C(38)	100.3(3)
I(3)−Rh(2)−N(2)	90.7(2)	I(3)−Rh(3)−N(9)	98.9(2)
I(3)−Rh(2)−N(4)	95.6(2)	I(3)−Rh(3)−N(11)	97.7(2)
I(3)−Rh(2)−C(17)	95.8(3)	I(3)−Rh(3)−C(33)	85.3(3)
I(3)−Rh(2)−C(22)	91.2(3)	I(3)−Rh(3)−C(38)	90.3(3)
N(2)−Rh(2)−N(4)	87.0(3)	N(9)−Rh(3)−N(11)	87.6(3)
N(2)−Rh(2)−C(17)	172.6(4)	N(9)−Rh(3)−C(33)	175.9(4)
N(2)−Rh(2)−C(22)	89.2(3)	N(9)−Rh(3)−C(38)	91.9(4)
N(4)−Rh(2)−C(17)	89.0(3)	N(11)−Rh(3)−C(33)	91.8(4)
N(4)−Rh(2)−C(22)	172.3(3)	N(11)−Rh(3)−C(38)	172.0(4)
C(17)−Rh(2)−C(22)	94.0(4)	C(33)−Rh(3)−C(38)	88.1(5)
Rh(2)−I(3)−Rh(3)	129.99(4)		

[a] For comparison, each column collects related geometrical parameters for each analogous, but crystallographically independent, dinuclear moiety "$Rh_2(\mu\text{-}Pz)_2(I)(CNBu^t)_4$".

and 2.766(6) Å)[20] and $[Rh_2(\mu\text{-}3,5\text{-}Me_2Pz)(I)_2(CO)_2(\mu\text{-}dppm)_2]^+$ (2.757(2) Å)[21] where the iodine atoms are *trans* disposed to the Rh−Rh bond. Nevertheless, both Rh−I distances are significantly longer than the average values observed for terminal or bridging iodide ligands in rhodium(III) complexes (2.71(7) and 2.73(1) Å, respectively),[22] probably as a consequence of the structural *trans*-effect associated to the metal−metal bonds.[23] The unusual coordination mode of the bridging iodide represents the first case in Rh or Ir chemistry where a iodine atom acts as the only ligand connecting two nonbonded metals. The unexpected value of the Rh−I−Rh bond angle, 129.99(4)°, probably represents a compromise between the general tendency observed when a single iodine atom acts as the sole bridging ligand between nonbonded metals in molecular crystals, with reported values close to an ideal sp^3 hybridization (109.5°),[22] and the strong steric requirements of the ligands bonded to bridged metals, Rh(2) and Rh(3).

The terminal *tert*-butyl isocyanide groups exhibit Rh−C bond distances in the range 1.896(11)−1.958(12) Å (mean 1.925(8) Å) and maintain linear dispositions around the coordinated carbon atoms (mean Rh−C−N, 174.1(7)°). These bonding parameters compare well with those reported for two closely related rhodium(II) dimers $[Rh_2(\mu\text{-}Pz)(Cl)_2(CNBu^t)_2(\mu\text{-}dppm)_2]^+$ (Rh−C, 1.933(5) and 1.940(5) Å; Rh−C−N, 176.3(4) and 172.8(5)°)[24] and $[Rh_2(\mu\text{-}Pz)(I)_2(CNBu^t)_2(\mu\text{-}dppm)_2]^+$ (Rh−C, 1.92(2) and 1.90(2) Å; Rh−C−N, 176.3(16) and 175.6(16)°),[20] where the isocyanide ligands are also *trans* disposed to bridging pyrazolate groups. The values reported in the latter two compounds for the Rh−N(pyrazolate) bonds are 2.069(5) and 2.067(5) Å[24] and 2.056(12) and 2.054(11) Å,[20] also in a good agreement with the bond distances determined in [**8**]$^+$, in the range 2.028(7)-2.061(8) Å (mean 2.039(4) Å). However, if compared with the rhodium(I) parent compound $[Rh(\mu\text{-}Pz)(CNBu^t)_2]_2$ (*av.* Rh−C 1.889(4); Rh−N 2.084(2) Å)[1] or the related complex $[(cod)Rh(\mu\text{-}Pz)_2Rh(CNBu^t)_2]$ (*av.* Rh−C 1.883(8); Rh−N 2.069(4) Å),[1] these distances reflect the different (lower) electronic density of the metals, which causes slightly longer Rh−C and shorter Rh−N bond distances in [**8**]$^+$.

Electronic Structure of *Folded* Binuclear Rh(II)−Rh(II) Species. In an attempt to gain insight into the intermetallic bonding system changes occurring on the binuclear rhodium species along the oxidative addition of diiodine to **1**, we have examined the electronic structures of several potential intermediates at a qualitative level.

The electronic structure of dirhodium(II) complexes (formally Rh_2^{4+}) has been extensively studied at different sophistication levels from a theoretical point of view using different approaches[25−32] and have been usually contrasted and complemented with photoelectronic or ESR spectroscopic experiments.[33−36] However, most of these studies have been concentrated on complexes of the *face-to-face* type where the two metals, bridged by four bidentate ligands, maintain their coordination planes practically parallel. For these rhodium lantern-type complexes, most of them containing bridging O-donor ligands and no axial groups (or with weak σ-donor as axial ligands), it now seems to be accepted that there

(20) Carmona, D.; Oro, L. A.; Pérez, P. L.; Tiripicchio, A.; Tiripicchio-Camellini, M. *J. Chem. Soc., Dalton Trans.* **1989**, 1427.
(21) Oro, L. A.; Carmona, D.; Pérez, P. L.; Esteban, M.; Tiripicchio, A.; Tiripicchio-Camellini, M. *J. Chem. Soc., Dalton Trans.* **1985**, 973.
(22) Allen, F. H.; Davies, J. E.; Galloy, J. J.; Johnson, O.; Kennard, O.; Macrae, C.F.; Mitchell, E. M.; Mitchell, G. F.; Smith, J. M.; Watson, D. G. *J. Chem. Inf. Comput. Sci.* **1991**, *31*, 187.
(23) Laguna, A.; Laguna, M.; Jiménez, J.; Lahoz, F. J.; Olmos, E. *J. Organomet. Chem.* **1992**, *435*, 235.
(24) Tortorelli, L. J.; Woods, C.; McPhail, A. T. *Inorg. Chem.* **1990**, *29*, 2726.
(25) Bursten, B. E.; Cotton, F. A. *Inorg. Chem.* **1981**, *20*, 3042.
(26) Le, J. C.; Chavan, M. Y.; Chau, L. K.; Bear, J. L.; Kadish, K. M. *J. Am. Chem. Soc.* **1985**, *107*, 7195.
(27) Poblet, J. M.; Benard, M. *Inorg. Chem.* **1988**, *27*, 2935.
(28) Bear, J. L.; Yao, C.-L.; Liu, L.-M.; Capdevielle, F. J.; Korp, J. D.; Albright, T. A.; Kang, S.-K.; Kadish, K. M. *Inorg. Chem.* **1989**, *28*, 1254.
(29) Kawamura, T.; Katayama, H.; Nishikawa, H.; Yamabe, T. *J. Am. Chem. Soc.* **1989**, *111*, 8156.
(30) Cotton, F. A.; Feng, X. *Inorg. Chem.* **1989**, *28*, 1180.
(31) Natkaniec, L.; Pruchnik, F. P. *J. Chem. Soc., Dalton Trans.* **1994**, 3261.
(32) Boyd, D. C.; Connelly, N. G.; Herbosa, G. G.; Hill, M. G.; Mann, K. R.; Mealli, C.; Orpen, A. G.; Richardson, K. E.; Rieger, P. H. *Inorg. Chem.* **1994**, *33*, 960.
(33) Kawamura, T.; Fukamachi, K.; Sowa, T.; Hayashida, S.; Yonezawa, T. *J. Am. Chem. Soc.* **1981**, *103*, 364.
(34) Rizzi, G. A.; Casarin, M.; Tondello, E.; Piraino, P.; Granozzi, G. *Inorg. Chem.* **1987**, *26*, 3406.
(35) Best, S. P.; Clark, R. J. H.; Nightingale, A. J. *Inorg. Chem.* **1990**, *29*, 1383.
(36) Stranger, R.; Medley, G. A.; McGrady, J. E.; Garret, J. M.; Appleton, T. G. *Inorg. Chem.* **1996**, *35*, 2268.

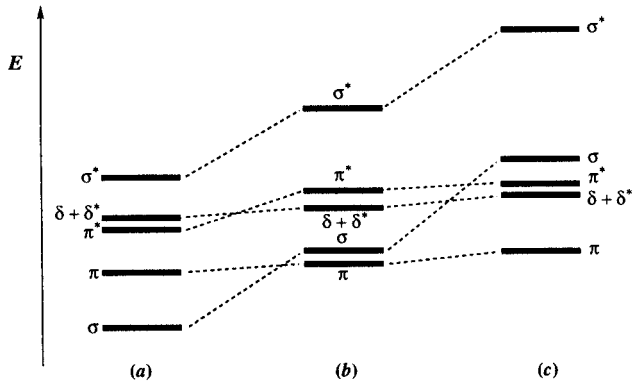

Figure 2. Molecular orbital diagram calculated for the species (a) $[Rh_2(\mu\text{-}Pz)_2(CNBu^t)_4]^{2+}$, (b) $[Rh_2(\mu\text{-}Pz)_2(I)(CNBu^t)_4]^{+}$, and (c) $[Rh_2(\mu\text{-}Pz)_2(I)_2(CNBu^t)_4]$.

exists a single σ metal−metal bond, corresponding to the usual electronic configuration $\sigma^2\pi^4\delta^2\delta^{*2}\pi^{*4}$ for the Rh_2^{4+} unit.[27] With strong σ-donors as the axial ligands, the σ level is strongly destabilized and it could become the HOMO.[25,31,35] In any case, the only unoccupied metal−metal orbital is the antibonding σ^*, leading to an intermetallic bond order of one.[28−30]

The substitution of bridging O-donor ligands by bidentate N-donor groups causes the δ^* and σ levels to rise in energy, while π and π^* are partially stabilized, resulting in an electronic configuration for the Rh_2^{4+} unit of $\sigma^2\pi^4\delta^2\pi^{*4}\delta^{*2}$, with the σ and π levels quite close in energy. These changes arise from the increased donor ability of the nitrogen atoms and the absence of the oxygen lone pairs which were responsible for the destabilization of the π and π^* orbitals.[28−30,34]

In our analysis, based on extended Hückel molecular orbital (EHMO) calculations, we have studied the electronic structure of the dication $[Rh_2(\mu\text{-}Pz)_2(CNBu^t)_4]^{2+}$ first. Using a simplified and symmetric model based on the solid state geometry observed for [**8**]$^+$ (see Experimental Section), we have carried out our calculations on a Rh(II)−Rh(II) binuclear species (formally Rh_2^{4+}) without any axial iodide ligand. The relative energy order of the intermetallic MOs (Figure 2a) is similar to those reported for the *face-to-face* type complexes, except for the δ and δ^* levels which become nearly degenerate. This situation is probably due to the folded geometry of our compounds, which exhibit the two metal coordination planes not parallel ($\alpha = 44°$),[1] and to the comparatively increased metal−metal distance. These geometrical constraints restrain the overlap among all orbitals of the two metal centers but affect to a greater extent the δ orbitals. Additionally, these two orbitals (δ, δ^*) are also destabilized by combination with the pyrazolate π orbitals. In spite of the commented differences, the electronic configuration for Rh_2^{4+}, $\sigma^2\pi^4\pi^{*4}\delta^2\delta^{*2}$, maintains an empty σ^* orbital, and hence, a single metal−metal bond should be also present in the examined binuclear moiety. As a point of reference, the calculated Mulliken population between both metals, 0.21 e$^-$, also reflects the intermetallic bond.

Further interaction of the two iodides as axial ligands with the binuclear entity $[Rh_2(\mu\text{-}Pz)_2(CNBu^t)_4]^{2+}$ modifies the electronic structure of the binuclear moiety to a situation very similar to that described by Cotton *et al.* for the adducts formed by tetrakis(carboxylato)-dirhodium(II) complexes and strong σ-donors.[25] As the iodide ligands approach the two metals, the metallic σ orbital mixes with the p_σ orbitals of the iodides, giving rise to a low-energy totally-bonding orbital and a second high-energy orbital with metal−metal bonding and metal−iodide antibonding character (Figures 3a and 3c, respectively), the latter one becoming the HOMO of the molecule. As these two new MOs are fully occupied, they do not substantially contribute to the metal−halogen bond order. On the other hand, the antisymmetric combination of the iodide p_σ orbitals with the empty metallic σ^* orbital forms an occupied low-energy orbital with a metal−metal antibonding and metal−halogen bonding character (Figure 3b) and a completely empty antibonding orbital (Figure 3d).[37] From these qualitative considerations, we can assume in a Mulliken sense a bonding order of 0.5 for the Rh−I bond. This fact explains the lability of acetonitrile or iodide groups when bonded as axial ligands in **5** or **3** and the particularly long Rh−I distances determined in the X-ray analysis of [**8**]$^+$. It is quite remarkable to note how the MO arrangement occurring when the binuclear species $[Rh_2(\mu\text{-}Pz)_2(CNBu^t)_4]^{2+}$ adds two axial iodides does not substantially modify the Rh−Rh bonding system (Mulliken population: 0.21−0.27 e$^-$) but it stabilizes the M−axial ligand interaction through the formation of a relatively weak bond. That is, in other words, the electronic basis of the commonly referred strong structural *trans*-effect of the σ Rh−Rh bonds.

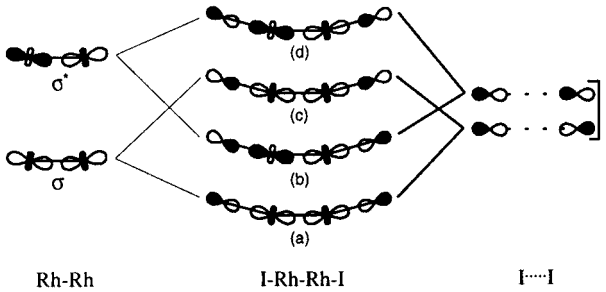

Figure 3. Schematic interaction diagram of the I−Rh−Rh−I σ-axial bonding system calculated from the interaction of $[Rh_2(\mu\text{-}Pz)_2(CNBu^t)_4]^{2+}$ with two axial iodide anions. Only level d is empty.

The most interesting results are obtained when the monocationic asymmetric $[Rh_2(\mu\text{-}Pz)_2(I)(CNBu^t)_4]^{+}$ moiety is analyzed. From a qualitative point of view, the σ and σ^* metal orbitals interact with an axial ligand donor function, giving up a totally-bonding, a totally-antibonding, and a nonbonding orbital.[28] Our EHMO calculation shows that this intermediate level presents a slight metal−metal bonding and metal−halogen antibonding character and additionally a large polarization toward the formally pentacoordinated rhodium atom (Figure 4): 68% of the electron density is concentrated on this atom, 6% on the octahedral rhodium atom, and 14% on the iodine ligand. A similar polarization of the Rh−Rh bond has been observed in the analysis of $[Rh_2\{(NH)_2CH\}_4(CH_3CN)]^{+}$ [28] and $[Rh_2(tcl)_4(CO)]^{+}$ (tcl = ω-thiocaprolactamate).[27] This electron transfer along the I−Rh−Rh system leads to a dramatic difference in the calculated Mulliken charges for the metal atoms: +0.67 e$^-$ for that linked to the halogen and +0.28 e$^-$ for the pentacoor-

(37) The performed calculations also identify the interactions between the π and π^* metal orbitals with those of the iodide ligands of appropiate symmetry (p_π). However, all of the resulting molecular orbitals are under the HOMO level, making their influence in the Rh−Rh or Rh−I bonding system negligible (see ref 31).

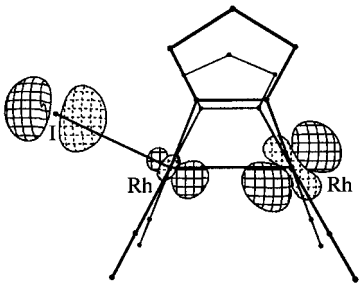

Figure 4. Cacao drawing of the "nonbonding" σ orbital of the I−Rh−Rh system.

dinated one. As a reference, the calculated charge for the symmetric compound with two axial iodo ligands is around +0.38 e^-. This polarization induces a partial disproportionation of the dirhodium Rh(II)−Rh(II) core toward an asymmetric structure. Hence, the metal−metal bond could be described as a dative bond from the pentacoordinated to the octahedral metal (formally I−Rh(III)−Rh(I)). In this situation, the cationic species $[Rh_2(\mu\text{-}Pz)_2(I)(CNBu^t)_4]^+$ seems to be susceptible of nucleophilic attack at the terminal pentacoordinated metal center: the coordination vacancy present together with the remaining positive charge (+0.28 e^-) support this proposal.

This description allows an easy understanding of the formation of the tetranuclear cation [**8**]$^+$ through a nucleophilic attack of the binuclear complex $[Rh_2(\mu\text{-}Pz)_2(I)_2(CNBu^t)_4]$ to the cationic species $[Rh_2(\mu\text{-}Pz)_2(I)(CNBu^t)_4]^+$.

Addition of Electrophiles to the Metal−Metal Bond. Reactions of **3** and **4** with 1 molar equiv of diiodine give the corresponding M(III)-M(III) complexes analyzing as $[\{M(\mu\text{-}Pz)(I)_2(CNBu^t)_2\}_2]$, which are isolated as air-stable red and orange crystalline solids, respectively. A formal oxidation of the starting M(II)−M(II) complexes is evidenced by the shift of ν(CN) by *ca.* 50 cm^{-1} to higher frequencies. The C_{2v} symmetry of the complexes, deduced from the ^1H and $^{13}C\{^1H\}$ NMR spectra, agrees with a boat conformation of the six-membered $Rh_2(N\text{-}N)_2$ ring, but the low solubility of these compounds in polar solvents makes the conductivity measurements inconclusive. However, they should be formulated as $[\{M(\mu\text{-}Pz)(I)(CNBu^t)_2\}_2(\mu\text{-}I)]I$ (M = Rh, [**9**]I; Ir, [**10**]I), i.e., ionic and containing just three bridging ligands because of their reactions with methyl triflate, which indicate their ionic nature. Thus, the formation of MeI is observed immediately after mixing [**9**]I and [**10**]I with $MeCF_3SO_3$, while the resonances for the cations remain unalterated. On a preparative scale, the resulting rhodium complex $[\{Rh(\mu\text{-}Pz)(I)(CNBu^t)_2\}_2(\mu\text{-}I)]CF_3SO_3$ ([**9**]CF_3SO_3) is isolated in good yield. Complex [**9**]CF_3SO_3 shows identical spectroscopic features to [**9**]I except for those of the anion and behaves as a 1:1 electrolyte in nitromethane.

To understand the pathway for the breaking of the metal−metal bond in the M(II)−M(II) complexes, we reacted the chloro derivative complex **7** with 1 molar equiv of diiodine. This allows us to determine the fate of the halide ligand (Cl) and the added halogen. The reaction is completed in 5 min in dichloromethane, and the ^1H and $^{13}C\{^1H\}$ NMR spectra of the crude orange solid, isolated by evaporation of the solvent to dryness, show the presence of three complexes, namely $[\{Rh(\mu\text{-}Pz)(Cl)(CNBu^t)_2\}_2(\mu\text{-}I)]^+$ ([**11**]$^+$; C_{2v}), $[Rh_2(\mu\text{-}Pz)_2(\mu\text{-}I)(I)(Cl)(CNBu^t)_4]^+$ ([**12**]$^+$; C_s), and $[\{Rh(\mu\text{-}Pz)(I)(CNBu^t)_2\}_2(\mu\text{-}I)]^+$ ([**9**]$^+$). Figure 5 shows the MS (FAB$^+$) of this mixture of complexes. Noticeably, the terminal halogen ligands are ionized in the mass spectrometer, but the bridging iodo ligand remains strongly attached in the cations, which is an additional useful observation to characterize the compounds.

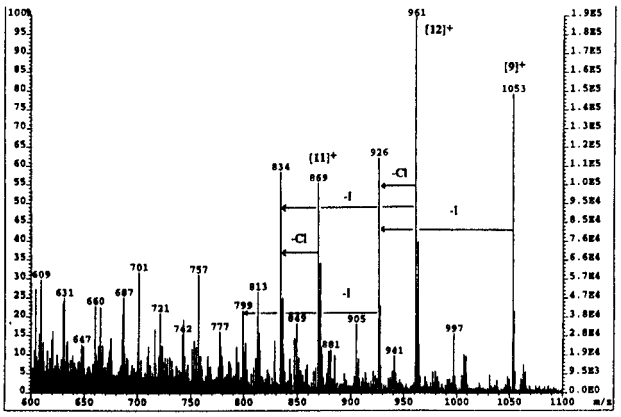

Figure 5. Mass spectrum from the reaction mixture of complex **7** with I_2, showing the peaks for the cations [**9**]$^+$, [**11**]$^+$, and [**12**]$^+$ and the losses of halide.[39]

The cations [**12**]$^+$ and [**9**]$^+$ result from a gradual replacement of the chloro ligands in [**11**]$^+$ by the iodide present in the reaction medium. Thus, the formation of [**11**]$^+$ is confirmed by carrying out the reaction of **7** with diiodine followed by the addition of methyltriflate, which removes the ionic iodide. Furthermore, the replacement of the chloro ligands in [**11**]$^+$ and [**12**]$^+$ by iodide, to give [**9**]$^+$, is immediate on addition of KI to the above solution in acetone-d_6. The lability of the halogen ligands in Rh(III) species has already been observed by Collman.[2] In conclusion, the reaction of **7** with diiodine initially leads to [**11**]I, a complex with an iodide ligand bridging the metals formerly bonded in the starting material.

Tentative Mechanism for the Rupture of the Metal−Metal Bond by Electrophiles. The addition of a iodine atom to the metal−metal bond in the pocket of complex of **7** is indicative of a selective reaction pathway, since six isomers could result from this reaction. On the other hand, the oxidation of **7** by diiodine is chemically inaccessible, since the cyclic voltammetry of **7** shows an irreversible oxidation peak at 1334 mV (*vs* SCE) in CH_2Cl_2, a value much larger than that for diiodine.[38] Therefore, a reaction pathway other than a direct electron transfer should be proposed.

The reaction of diiodine with **7**, as well as with **3** and **4**, can be envisaged as the addition of one halogen atom at the metal−metal bond. A reasonable mechanism requires the interaction of a diiodine molecule with the electronic density in the M−M metal bond, as shown in Scheme 3 for **7**. This hypothetical transition state (**B**) could lead to the heterolytic cleavage of the I−I bond, resulting in an iodide ligand bridging two rhodium atoms, i.e., the cation [**11**]$^+$ and an iodide anion. This proposal involves the actuation of both metals in a cooperative way, such that the metal−metal bond is acting as a nucleophile. The transition state resembles

(38) Connelly, N. G.; Geiger, W. E. *Chem. Rev.* **1996**, *96*, 877.
(39) The isotopic profile of the peak at 777 does not correlate to that calculated for the cation $[C_{26}H_{42}N_8Cl_3Rh_2]^+$.

Scheme 3

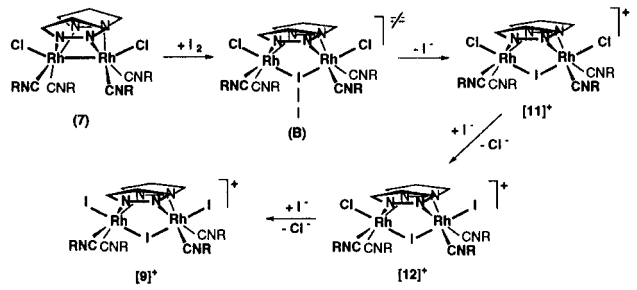

Scheme 4

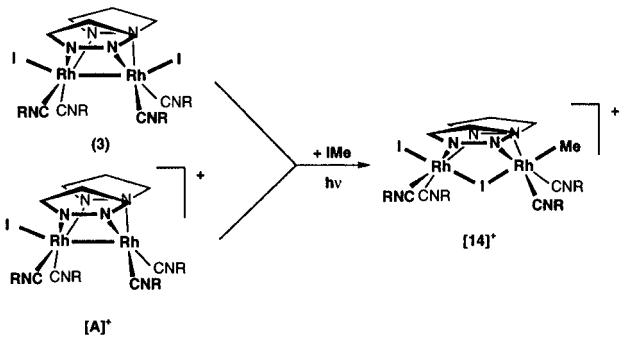

that proposed for the electrophilic additions of iodine to carbon−carbon double bonds.

Definitive support for the nucleophilic attack by the metal−metal bond to the diiodine molecule leading to heterolytic rupture of the I−I bond comes from the reactions of **3**, **4**, and noticeably **7** with the cationic complex $[I(Py)_2]BF_4$, which possesses a positive iodine atom. They quantitatively give the complexes [**9**]BF_4, [**10**]BF_4, and [**11**]BF_4, respectively, and pyridine (Py) (^{1}H NMR evidence) in which the added iodine(I) bridges the rhodium atoms.

According to the proposed mechanism, complex **3** should react with organoiodo compounds in which the iodine atom possesses a small positive charge, such as I−C≡C−Ph.[40] This reaction gives an orange-brown solid analyzing as $[(CNBu^t)_2(I)Rh(\mu\text{-}Pz)_2(\mu\text{-}I)Rh(\eta^1\text{-}C{\equiv}C{-}Ph)(CNBu^t)_2]I$ ([**13**]I). The ^{1}H and $^{13}C\{^1H\}$ NMR spectra of the solid indicate that [**13**]I is contaminated by small amounts of two other products possessing C_{2v} symmetry. One of them is $[\{Rh(\mu\text{-}Pz)(I)(CNBu^t)_2\}_2(\mu\text{-}I)]I$ ([**7**]I), identified by comparison of the spectra with those of the characterized compound, and the other probably corresponds to the dialkynyl cation $[\{Rh(\mu\text{-}Pz)(\eta^1\text{-}C{\equiv}CPh)(CNBu^t)_2\}_2(\mu\text{-}I)]^+$. The terminal η^1-coordination of the alkynyl group in [**13**]$^+$ is deduced from the C_s symmetry of the complex, along with the observation of two acetylenic carbons in the $^{13}C\{^1H\}$ NMR spectrum distinctively coupled with a single ^{103}Rh nucleus.[41]

The reaction between **3** and I−C≡C−Ph should occur via the nucleophilic attack of the metal−metal bond to the positive iodine atom, following the halogen transfer, to give [**9**]$^+$ and Ph−C≡C$^-$ as the counteranion. Indeed, complex [**9**]$^+$ is the initial product observed by monitoring the reaction by ^{1}H NMR spectroscopy. Phenylacetelyde reacts further with [**9**]$^+$ replacing one or two terminal iodide ligands to give the observed mixture, essentially containing [**13**]$^+$ and small equimolecular amounts of [**9**]$^+$ and $[\{Rh(\mu\text{-}Pz)(\eta^1\text{-}C{\equiv}CPh)(CNBu^t)_2\}_2(\mu\text{-}I)]^+$.

As expected from this mechanism, complex **3** does not react with MeI in the dark, since the iodine atom supports a partial negative charge in the I−C_{sp^3} bond and the methyl group is not electrophilic enough to interact with **3**. In summary, complex **3** reacts at the exo site with a strongly electrophilic methyl group such as $MeCF_3SO_3$, while the endo site, i.e., the metal−metal bond in **3**, is the preferred position for iodine and electrophilic iodine compounds.

Photochemical Reactions Leading to the Rupture of the Metal-Metal Bond. Although the dinuclear cation [**A**]$^+$ is prone to add a donor from the medium at the vacant coordination position, our attempts to isolate M(η^1-XR) halocarbon adducts[42] of this cation with the iodo derivatives MeI and PhI result in irresolvable oils. However, we were surprised that [**A**]$^+$ in MeI gave rise to the oxidative-addition product $[(CNBu^t)_2(I)Rh(\mu\text{-}Pz)_2(\mu\text{-}I)Rh(Me)(CNBu^t)_2]CF_3SO_3$ ([**14**]CF_3SO_3) (Scheme 4) in 60% yield in 1 week. Characterization of ([**14**]CF_3SO_3) relies on the analytical and spectroscopic data, and NOE experiments are conclusive to localize the methyl group outside the pocket of the complex.

As the addition of MeI to the cation ([**A**]$^+$) is unlikely, we investigated this reaction further to find that it actually requires the irradiation with the direct sunlight or with an intense visible lamp. Examination of the crude product revealed the presence of [**14**]CF_3SO_3 as the main component, along with [**9**]CF_3SO_3 and $[(CNBu^t)_2(Me)Rh(\mu\text{-}Pz)_2(\mu\text{-}I)Rh(Me)(CNBu^t)_2]CF_3SO_3$ ([**15**]CF_3SO_3) as impurities. One can speculate that the adduct of MeI with the dinuclear cation [**A**]$^+$ could be the intermediate for an inner-sphere electron transfer, although it is not actually a typical decomposition pathway taken by halocarbon complexes.[43] However, this hypothesis was ruled out because irradiation of complex **3** in MeI under identical conditions as those above gives [**14**]I even more cleanly. Small amounts (<10%) of [**8**]I and [**15**]I are also found in the crude product.

The UV−vis spectrum of **3** shows two absorption bands in the visible region at λ = 450 and 395 nm. Absorption bands in this region have been assigned to a dσ−dσ* transition from the dσ^2 ground state of the $d^7{}_2$ configuration systems.[44] Therefore, the triplet excited state dσ^1dσ^{*1} is easily reached on irradiation, and this excited species should react with MeI. Surprisingly, a high selectivity is observed for this photochemical reaction.

Conclusions

The complexes $[\{M(\mu\text{-}Pz)(CNBu^t)_2\}_2]$ (M = Rh (**1**), Ir (**2**); Pz = pyrazolate) are capable of recognizing the different nature of their reactions with MeI and diiodine,

(40) (a) Ghassemzadeh, M.; Harms, K.; Dehnicke, K. *Chem. Ber.* **1996**, *129*, 115. (b) Davies, J. A.; El-Ghanam, M.; Pinkerton, A. A.; Smith, D. A. *J. Organomet. Chem.* **1991**, *409*, 367.

(41) Werner, H.; Wiedemann, R.; Mahr, N.; Steinert, P.; Wolf, J. *Chem. Eur. J.* **1996**, *2*, 561.

(42) (a) Butts, M. D.; Scott, B. L.; Kubas, G. J. *J. Am. Chem. Soc.* **1996**, *118*, 11831. (b) Kulawiec, R. J.; Crabtree, R. H. *Coord. Chem. Rev.* **1990**, *99*, 89.

(43) Peng, T.-S.; Winter, C. H.; Gladysz, J. A. *Inorg. Chem.* **1994**, *33*, 2534.

(44) Bailey, J. A.; Grundy, S. L.; Stobart, S. R. *Inorg. Chim. Acta* **1996**, *243*, 47.

since they give the M(III)−M(III) complexes either through the mixed-valence M(I)−M(III) intermediates or through the metal−metal-bonded complexes, respectively. Our findings could be explained because of two different properties, the nucleophilic and the reductor characteristics of **1** and **2**. It should be mentioned that, in some instances, both substrates have been considered alike for oxidative-addition reactions because they give apparently analogous results.

The separation of an oxidative-addition reaction across two metal atoms into two formal steps, the chemical oxidation and the capture of the additional ligands, indicates that this type of reaction is an electron-transfer reaction. Once the oxidative-addition reaction has been carried out, two reactive sites available for reactions with electrophiles remain in the molecules $[\{M(\mu\text{-Pz})(X)(CNBu^t)_2\}_2]$ (X = Cl, I). These are the metal−metal bond and the halogen ligands at the *trans* positions. The reactions of these complexes with diiodine leading to the breaking of the metal−metal bond involve the electron density at this site, which should act as a nucleophile. Probably the metal−metal bond polarizes the diiodine molecule producing its heterolytic cleavage. This proposal is supported by the reaction of the complex $[\{Rh(\mu\text{-Pz})(I)(CNBu^t)_2\}_2]$ (**3**) with the iodine(I) complex $[I(Py)_2]^+$ at the metal−metal bond leaving the iodine atom bridging the metal atoms.

The terminal halogen ligands in $[\{Rh(\mu\text{-Pz})(I)(CNBu^t)_2\}_2]$ are abstracted by strong electrophiles, such as $MeCF_3SO_3$, to give the binuclear cationic complex $[Rh_2(\mu\text{-Pz})_2(I)(CNBu^t)_4]^+$ (**A**$^+$). Notice that the latter reaction leads to an important change in the nucleophilicity of the metallic centers compared with complexes **1** and **3**. EHMO calculations for this cation reveal an uneven distribution of the electron density on the metals, resulting in a polarized Rh−Rh bond. This polarization induces a partial disproportionation of the dirhodium core toward an asymmetric structure, and the metal−metal bond is best described as a dative bond from the pentacoordinated metal to the octahedral metal (formally I−Rh(III)−Rh(I)).

A second pathway to break the metal−metal bond is a photochemically assisted addition. The visible light should promote an electron from the $d\sigma^2$ ground state of the $d^7{}_2$ configuration to an excited state $d\sigma^1 d\sigma^{*1}$. The metal−metal bond is broken in the excited state, and hence, a structure with a large metal−metal separation should be the reactive species

Experimental Section

All reactions were carried out under argon using standard Schlenk techniques. The complexes $[\{M(\mu\text{-Pz})(CNBu^t)_2\}_2]$ (M = Rh, **1**; Ir, **2**) were prepared according to literature methods.[1] Solvents were dried and distilled under argon before use by standard methods. For additional general information, including a list of the spectrophotometers and equipment used for the physical characterization, see ref 1.

Preparation of the Complexes. $[\{Rh(\mu\text{-Pz})(I)(CNBu^t)_2\}_2]$ (3). Addition of solid I_2 (37.7 mg, 0.15 mmol) to a yellow solution of $[\{Rh(\mu\text{-Pz})(CNBu^t)_2\}_2]$ (**1**) (100 mg, 0.15 mmol) in acetone (20 mL) immediately produces an orange solution. The solution was stirred for 30 min in the dark and concentrated to *ca.* 2 mL. Slow addition of diethyl ether (15 mL) to the evaporated solution rendered compound **3** as orange neddles, which were filtered, washed with cold diethyl ether, and dried under vacuum. Yield: 127 mg (92%). Anal. Calcd for $C_{26}H_{42}N_8I_2Rh_2$: C, 33.71; H, 4.57; N, 12.10. Found: C, 33.67; H, 4.28; N, 12.35. IR (CH_2Cl_2, cm^{-1}): ν(CN) 2199 (s), 2173 (s). ^{1}H NMR (room temperature, $CDCl_3$): δ 7.59 (d, J = 1.9 Hz, 4H, H^{3,5}Pz), 5.96 (t, J = 1.9 Hz, 2H, H^{4}Pz), 1.47 (s, 36H, CNBu^t). ^{13}C{^{1}H} NMR (room temperature, $CDCl_3$): δ 138.7 (C^{3,5}Pz), 138.0 (d, $^1J_{RhC}$ = 56 Hz, *C*NBu^t), 104.5 (C^{4}Pz), 58.4 (*C*-(CH$_3$)$_3$), 30.8 (C-(*C*H$_3$)$_3$). MS (FAB$^+$, CH_2Cl_2, *m*/*z*): 742 (10, M$^+$), 707 (100, M − I$^+$), 672 (40, M − 2I$^+$), 1449 (10, 2M − I$^+$).

$[\{Ir(\mu\text{-Pz})(I)(CNBu^t)_2\}_2]$ (4) was prepared as described for **3**, starting from **2** (75 mg, 0.09 mmol) and I_2 (22.4 mg, 0.09 mmol) to give a yellow-orange solid, which was recrystallized twice from CH_2Cl_2/diethyl ether to render yellow neddles of **4**, which were isolated by filtration. Yield: 70 mg (72%). Anal. Calcd for $C_{26}H_{42}N_8I_2Ir_2$: C, 28.26; H, 3.83; N, 10.14. Found: C, 28.35; H, 3.88; N, 10.18. IR (CH_2Cl_2, cm^{-1}): ν(CN) 2189 (s), 2151 (s). ^{1}H NMR (room temperature, $CDCl_3$): δ 7.45 (d, J = 1.9 Hz, 4H, H^{3,5}Pz), 5.87 (t, J = 1.9 Hz, 2H, H^{4}Pz), 1.45 (s, 36H, CNBu^t). ^{13}C{^{1}H} NMR (room temperature, $CDCl_3$): δ 138.5 (C^{3,5}Pz), 104.2 (C^{4}Pz), 58.0 (*C*−(CH$_3$)$_3$), 31.4 (C−(*C*H$_3$)$_3$). MS (FAB$^+$, CH_2Cl_2, *m*/*z*): 1104 (56, M$^+$), 977 (100, M − I$^+$), 1998 (6, 2M − I − CNBu^{t+}).

$[\{Rh(\mu\text{-Pz})(CNBu^t)_2(CH_3CN)\}_2](PF_6)_2$ ([5]$(PF_6)_2$). Solid $[Cp_2Fe]PF_6$ (99.5 mg, 0.30 mmol) was added to a solution of **2** (100 mg, 0.15 mmol) in dry acetonitrile (10 mL) to give a pale-orange solution almost immediately. After concentration to 1 mL, the addition of diethyl ether produces the precipitation of [**5**]$(PF_6)_2$. The solid was filtered, washed 3 × 10 mL of diethyl ether to remove the ferrocene, and vacuum dried. Yield: 140 mg (90%). Anal. Calcd for $C_{30}H_{48}N_{10}P_2F_{12}Rh_2$: C, 34.50; H, 4.63; N, 13.41. Found: C, 34.16; H, 4.27; N, 13.27. IR (CH_3CN, cm^{-1}): ν(CN) 2224 (s), 2203 (s). ^{1}H NMR (213 K, acetone-d_6) for $[\{Rh(\mu\text{-Pz})(CNBu^t)_2(MeCN)\}_2]^{2+}$: δ 7.71 (d, J = 1.7 Hz, 4H, H^{3,5}Pz), 6.22 (t, J = 1.7 Hz, 2H, H^{4}Pz), 2.75 (s, 9H, CH_3CN), 1.58 (s, 36H, CNBu^t); for $[\{Rh(\mu\text{-Pz})(CNBu^t)_2\}_2(MeCN)(Me_2CO)]^{2+}$: δ 7.77 (d, J = 1.7 Hz, 2H, H^3-Pz), 7.65 (d, J = 1.7 Hz, 2H, H^{5}Pz), 6.23 (t, J = 1.7 Hz, 2H, H^{4}Pz), 2.79 (s, 3H, CH_3CN), 1.61 and 1.56 (s, 18H + 18H, CNBu^t). ^{19}F NMR (213 K, acetone-d_6): δ 70.60 (d, J_{F-P} = 709 Hz, PF_6). MS (FAB$^+$, acetone, *m*/*z*): 817 (4, M − 2CH_3CN + PF_6^+), 672 (100, M − 2CH_3CN^+). Λ_M (4.9 × 10^{-4} M in acetone) = 232 S cm^2 mol^{-1}.

$[\{Ir(\mu\text{-Pz})(CNBu^t)_2(CH_3CN)\}_2](PF_6)_2$ ([6]$(PF_6)_2$) was prepared as described for **5**, starting from **2** (75 mg, 0.09 mmol) and $[Cp_2Fe]PF_6$ (58.9 mg, 0.18 mmol) to give white microcrystals of [**6**]$(PF_6)_2$. Yield: 100 mg (92%). Anal. Calcd for $C_{30}H_{48}N_{10}P_2F_{12}Ir_2$: C, 29.46; H, 3.96; N, 11.45. Found: C, 29.38; H, 3.53; N, 11.31. IR (CH_2Cl_2, cm^{-1}): ν(CN) 2218 (s), 2181 (s). ^{1}H NMR (213 K, acetone-d_6): δ 7.45 (d, J = 2.1 Hz, 4H, H^{3,5}Pz), 6.17 (t, J = 2.1 Hz, 2H, H^{4}Pz), 2.86 (s, 9H, CH_3-CN), 1.58 (s, 36H, CNBu^t). MS (FAB$^+$, acetone, *m*/*z*): 850 (100, M − 2CH_3CN^+). Λ_M (5.0 × 10^{-4} M in acetone) = 224 S cm^2 mol^{-1}.

$[\{Rh_2(\mu\text{-Pz})_2(I)(CNBu^t)_4\}_2(\mu\text{-I})]CF_3SO_3$ ([8]CF_3SO_3). To a solution of **3** (100 mg, 0.108 mmol) in acetone (10 mL), $MeCF_3SO_3$ (6 μL, 0.054 mmol) was added. The initial orange solution turns dark red in 10 min. The solution was concentrated to *ca.* 3 mL and carefully layered with 20 mL of diethyl ether to give dark red monocrystals with a green metallic luster, suitable for X-ray diffraction studies. The solid was filtered, washed with 2 × 10 mL of diethyl ether, and vaccum dried. Yield: 70 mg (69%). Anal. Calcd for $C_{53}H_{84}N_{16}I_3F_3SO_3Rh_4$: C, 33.95; H, 4.52; N, 11.95; S, 1.71. Found: C, 34.03; H, 4.46; N, 11.85; S, 2.06. MS (FAB$^+$, CH_2Cl_2, *m*/*z*): 1449 (10, M$^+$), 707 (100, M − [**3**]$^+$).

$[\{Rh(\mu\text{-Pz})(I)(CNBu^t)_2\}_2(\mu\text{-I})]I$ ([9]I). The addition of solid I_2 (38.1 mg, 0.15 mmol) to an acetone (15 mL) solution of $[\{Rh(\mu\text{-Pz})(I)(CNBu^t)_2\}_2]$ (**3**) (139 mg, 0.15 mmol) leads to the immediate precipitation of a red microcrystalline solid. After the mixture was stirred for 1 h, the suspension was concentrated to dryness. The residue was dissolved in 3 mL of dichloromethane and layered with pentane (20 mL) overnight

to render red prismatic crystals. The solution was decanted, and the crystals were washed with cold diethyl ether and vacuum dried. Yield: 174 mg (98%). Anal. Calcd for $C_{26}H_{42}N_8I_4Rh_2$: C, 26.46; H, 3.58; N, 9.49. Found: C, 26.39; H, 3.61; N, 9.32. IR (CH_2Cl_2, cm^{-1}): ν(CN) 2240 (s), 2219 (s). ^1H NMR (room temperature, $CDCl_3$): δ 8.05 (d, J = 2.2 Hz, 4H, $H^{3,5}$Pz), 6.13 (t, J = 2.2 Hz, 2H, H^4Pz), 1.61 (s, 36H, CNBu^t). $^{13}C\{^1H\}$ NMR (room temperature, $CDCl_3$): δ 145.5 ($C^{3,5}$Pz), 120.2 (d, $^1J_{RhC}$ = 45 Hz, *C*NBu^t), 107.0 (C^4Pz), 60.3 (*C*−$(CH_3)_3$), 30.2 (C−(*C*$H_3)_3$). MS (FAB$^+$, CH_2Cl_2, *m*/*z*): 1053 (100, M^+), 926 (55, M − I^+), 799 (12, M − 2I^+).

[{Rh(μ-Pz)(I)(CNBu^t)$_2$}$_2$(μ-I)]CF_3SO_3 ([9]CF_3SO_3). To a suspension of [**8**]I (100 mg, 0.085 mmol) in acetone (10 mL), $MeCF_3SO_3$ (10 μL, 0.085 mmol) was added to give an orange solution in 5 min. Concentration of this solution and layering with diethyl ether overnight gave orange microcrystals, which were isolated by filtration and washed with diethyl ether. Yield: 82 mg (79%). Anal. Calcd for $C_{27}H_{42}N_8I_3F_3SO_3Rh_2$: C, 26.97; H, 3.52; N, 9.32; S, 2.67. Found: C, 27.23; H, 3.58; N, 8.95; S, 2.45. ^{19}F NMR (room temperature, $CDCl_3$): δ −78.30 (s, CF_3SO_3). Λ_M (2.8 × 10^{-4} M in nitromethane) = 75 S cm^2 mol^{-1}. The ^1H and $^{13}C\{^1H\}$ NMR spectra, ν(CN), and mass spectrum are identical as those described for [**9**]I.

[{Ir(μ-Pz)(I)(CNBu^t)$_2$}$_2$(μ-I)]I ([10]I). The addition of solid I_2 (13.8 mg, 0.055 mmol) to an acetone (15 mL) solution of [{Ir(μ-Pz)(I)(CNBu^t)$_2$}$_2$] (**4**) (60 mg, 0.055 mmol) leads to an orange solution. Evaporation of this solution and layering with diethyl ether gave [**10**]I as orange cubic crystals. The solution was decanted, and the crystals were washed with cold diethyl ether and vacuum dried. Yield: 59 mg (80%). Anal. Calcd for $C_{26}H_{42}N_8I_4Ir_2$: C, 22.98; H, 3.12; N, 8.24. Found: C, 22.54; H, 2.50; N, 7.84. IR (CH_2Cl_2, cm^{-1}): ν(CN) 2232 (s), 2210 (s). ^1H NMR (room temperature, $CDCl_3$): δ 8.08 (d, J = 2.3 Hz, 4H, $H^{3,5}$Pz), 6.11 (t, J = 2.3 Hz, 2H, H^4Pz), 1.61 (s, 36H, CNBu^t). $^{13}C\{^1H\}$ NMR (room temperature, $CDCl_3$): δ 144.5 ($C^{3,5}$Pz), 107.3 (C^4Pz), 59.8 (*C*−$(CH_3)_3$), 30.6 (C−(*C*$H_3)_3$). MS (FAB$^+$, CH_2Cl_2, *m*/*z*): 1231 (100, M^+), 1104 (65, M − I^+), 977 (40, M − 2I^+).

[{Rh(μ-Pz)(Cl)(CNBu^t)$_2$}$_2$(μ-I)]BF_4 ([11]BF_4). The addition of solid [I(Py)$_2$]BF_4 (24.9 mg, 0.067 mmol) to an acetone (10 mL) solution of [{Rh(μ-Pz)(Cl)(CNBu^t)$_2$}$_2$] (**7**) (50 mg, 0.067 mmol) leads to an orange solution. Evaporation of this solution to 2 mL and layering with diethyl ether (15 mL) gave [**11**]BF_4 as orange microcrystals. The solution was decanted, and the crystals were washed with cold diethyl ether and vacuum dried. Yield: 50 mg (78%). Anal. Calcd for $C_{26}H_{42}N_8Cl_2IRh_2BF_4$: C, 32.63; H, 4.42; N, 11.70. Found: C, 32.57; H, 4.45; N, 11.44. IR (CH_2Cl_2, cm^{-1}): ν(CN) 2239 (s), 2231 (s). ^1H NMR (room temperature, $CDCl_3$): δ 7.75 (d, J = 2.3 Hz, 4H, $H^{3,5}$Pz), 6.23 (t, J = 2.3 Hz, 2H, H^4Pz), 1.60 (s, 36H, CNBu^t). $^{13}C\{^1H\}$ NMR (room temperature, $CDCl_3$): δ 141.5 ($C^{3,5}$Pz), 106.6 (C^4Pz), 60.6 (*C*-$(CH_3)_3$), 29.9 (C−(*C*$H_3)_3$). MS (FAB$^+$, CH_2Cl_2, *m*/*z* for ^{35}Cl): 869 (100, M^+), 834 (52, M − Cl^+), 799 (7, M − 2Cl^+). Λ_M (4.9 × 10^{-4} M in acetone) = 135 S cm^2 mol^{-1}.

Reaction of [{Rh(μ-Pz)(Cl)(CNBu^t)$_2$}$_2$] (7) with Iodine and Methyl Triflate. To a solution of **7** (70 mg, 0.095 mmol) in acetone were successively added solid I_2 (24 mg, 0.095 mmol) and $MeCF_3SO_3$ (11 μL, 0.095 mmol) after 5 min. The resulting orange solution was concentrated to 2 mL, and the extract was layered with 20 mL of diethyl ether overnight to give orange microcrystals. The solution was decanted, and the solid was washed with diethyl ether and vacuum dried. Yield: 80 mg. The crude solid contains 45% of [**11**]CF_3SO_3, 19% of [**9**]CF_3SO_3, and 36% of the new complex [Rh_2(μ-Pz)$_2$(I)(Cl)(CNBu^t)$_4$(μ-I)]CF_3SO_3 ([**12**]CF_3SO_3). ^1H NMR for [**12**]$^+$ (room temperature, $CDCl_3$): δ 8.06 (d, J = 2.2 Hz, 2H, H^3Pz), 7.74 (d, J = 2.2 Hz, 2H, H^5Pz), 6.19 (t, J = 2.2 Hz, 2H, H^4Pz), 1.60 and 1.59 (s, 18H + 18H, CNBu^t). $^{13}C\{^1H\}$ NMR for [**12**]$^+$ (room temperature, $CDCl_3$): δ 141.8 (C^3), 145.4 (C^5), 107.3 (C^4Pz), 60.7 (*C*−$(CH_3)_3$), 30.1 (C−(*C*$H_3)_3$). Complex [**9**]$^+$ pure results upon addition of KI to this mixture in $CDCl_3$ solution.

[(CNBu^t)$_2$(I)Rh(μ-Pz)$_2$(μ-I)Rh(η^1-C≡C−Ph)(CNBu^t)$_2$]I ([13]I). I−C≡C−Ph (40 mg, 0.17 mmol) was added to a solution of **3** (100 mg, 0.11 mmol) in dichloromethane (5 mL). The reaction was completed in 4 h at room temperature. Evaporation of the resulting solution to 1 mL and addition of diethyl ether (10 mL) rendered dark-orange crystals, which were separated by filtration, washed with diethyl ether, and vacuum dried. Yield: 91 mg (73%). Anal. Calcd for $C_{34}H_{47}N_8I_3Rh_2$: C, 35.38; H, 4.10; N, 9.71. Found: C, 35.38; H, 4.15; N, 9.88. IR (CH_2Cl_2, cm^{-1}): ν(CN) 2235 (s), 2220 (s). ^1H NMR (room temperature, $CDCl_3$): δ 8.08 (d, J = 2.1 Hz, 2H, H^3Pz), 7.76 (d, J = 2.1 Hz, 2H, H^5Pz), 7.30 (m, 5H, Ph), 6.17 (t, J = 2.1 Hz, 2H, H^4Pz), 1.66 and 1.61 (s, 18H + 18H, CNBu^t). $^{13}C\{^1H\}$ NMR (room temperature, $CDCl_3$): δ 145.2 (C^3Pz), 142.7 (C^5Pz), 131.6, 128.1, 126.7, and 126.0 (Ph), 106.9 (C^4Pz), 97.1 (d, $^2J_{C-Rh}$ = 8 Hz, Rh−C≡*C*−Ph), 81.0 (d, $^1J_{C-Rh}$ = 48 Hz, Rh−*C*≡C−Ph), 60.6 and 60.4 (*C*−$(CH_3)_3$), 30.3 (C−(*C*$H_3)_3$). MS (FAB$^+$, CH_2Cl_2, *m*/*z*): 1027 (100, M^+), 900 (52, M − I^+), 799 (31, M − I − C_2Ph^+). Λ_M (5.1 × 10^{-4} M in acetone) = 80 S cm^2 mol^{-1}.

[(CNBu^t)$_2$(I)Rh(μ-Pz)$_2$(μ-I)Rh(Me)(CNBu^t)$_2$]A ([14]A, A = CF_3SO_3, I). A solution of complex **3** (100 mg, 0.11 mmol) in MeI (2 mL) was treated with $MeCF_3SO_3$ (12 μL, 0.11 mmol) to give a purple solution. Irradiation for 2 h with a 400 W visible lamp or under direct sunlight gave an orange solution. Evaporation to dryness gave a crude solid containing 76% of [**14**]CF_3SO_3, which was extracted with acetone (3 mL). Addition of diethyl ether (10 mL) to the extract gave orange microcrystals, which were separated by decantation and washed with diethyl ether. Yield: 71 mg (60%). Anal. Calcd for $C_{28}H_{45}N_8I_2F_3SO_3Rh_2$: C, 30.84; H, 4.16; N, 10.27; S, 2.94. Found: C, 30.61; H, 3.88; N, 9.67; S, 2.81.

Irradiation of a solution of **3** (100 mg, 0.11 mmol) in MeI (2 mL) for 2 h with a 400 W visible lamp or under direct sunlight and evaporation to dryness gave a crude solid containing 81% of [**14**]I, which was recrystallized as described above. Yield: 75 mg (65%). Anal. Calcd for $C_{27}H_{45}N_8I_3Rh_2$: C, 30.35; H, 4.24; N, 10.49. Found: C, 30.58; H, 4.04; N, 10.34. IR (CH_2Cl_2, cm^{-1}): ν(CN) 2224 (s), 2205 (s). ^1H NMR (room temperature, $CDCl_3$): δ 8.07 (d, J = 2.1 Hz, 2H, H^3Pz), 7.30 (d, J = 2.1 Hz, 2H, H^5Pz), 6.17 (t, J = 2.1 Hz, 2H, H^4Pz), 1.83 (d, J_{H-Rh} = 2.1 Hz, 3H, Me−Rh), 1.58 and 1.57 (s, 18H + 18H, CNBu^t). $^{13}C\{^1H\}$ NMR (room temperature, $CDCl_3$): δ 145.2 (C^3Pz), 140.2 (C^5Pz), 106.8 (C^4Pz), 60.3 and 60.0 (*C*−$(CH_3)_3$), 30.3 and 30.1 (C−(*C*$H_3)_3$), 8.60 (d, J_{C-Rh} = 21 Hz, Me−Rh). MS (FAB$^+$, CH_2Cl_2, *m*/*z*): 941 (100, M^+), 926 (10, M − Me^+), 814 (45, M − I^+), 799 (8, M − I − Me^+). Λ_M (5.1 × 10^{-4} M in acetone) = 102 S cm^2 mol^{-1}.

Crystal Structure Determination of [{Rh$_2$(μ-Pz)$_2$(I)(CNBu^t)$_4$}$_2$(μ-I)]CF_3SO_3 ([8]CF_3SO_3). A summary of crystal data and refinement parameters is reported in Table 2. A dark-red prismatic crystal (0.50 × 0.44 × 0.32 mm) was used to collect data on a Siemens-P4 diffractometer with graphite-monochromated Mo Kα radiation (λ = 0.710 73 Å). Cell constants were obtained from the least-squares fit on the setting angles of 36 reflections in the range 16° ≤ 2θ ≤ 25°. Reflections with 2θ in the range 3−45° were measured using the ω/2θ scan technique and corrected for Lorentz and polarization effects. Reflections were also corrected for absorption by a semiempirical method (Ψ-scans, 12 reflections).[45] Three standard reflections were monitored every 97 measurements throughout data collection as a check of crystal and instrument stability; no important variation was observed.

The structure was solved by direct methods (SIR92)[46] and difference Fourier techniques and refined by full-matrix least-squares on F^2 (SHELXL93).[47] Anisotropic thermal parameters were used in the last cycles of refinement for all non-hydrogen

(45) North, A. C. T.; Phillips, D. C.; Mathews, F. S. *Acta Crystallogr., Sect. A* **1968**, *24*, 351.

(46) Altomare, A.; Cascarano, G.; Giacovazzo, C.; Guagliardi, A. *J. Appl. Crystallogr.* **1994**, *27*, 435.

(47) Sheldrick, G. M. *SHELXL-93*; University of Göttingen: Göttingen, Germany, 1993.

Table 2. Crystallographic Data and Structure Refinement for [8]CF_3SO_3

chem formula	$C_{53}H_{84}F_3I_3N_{16}O_3Rh_4S$
fw	1807.08
cryst syst	monoclinic
space group	$P2_1/c$ (No. 14)
a, Å	21.082(3)
b, Å	18.452(2)
c, Å	21.717(2)
β, deg	92.165(7)
V, Å^3	8442(2)
Z	4
μ, mm^{-1}	1.938
θ range of data collected, deg	1.5–22.5
index ranges	$-1 \le h \le 22$, $-1 \le k \le 19$, $-23 \le l \le 23$
no. of measd reflns	14 509
no. of unique reflns	10944 ($R_{int} = 0.0263$)
abs corr method	ψ-scan
min, max transmission factors	0.291, 0.347
no. of data/restraints/params	10940/170/671
$R(F)$ [$F^2 > 2\sigma(F^2)$][a]	0.0476 (6407 reflns)
w$R(F^2)$ [all data][b]	0.1421
S [all data][c]	0.921

[a] $R(F) = \sum||F_o| - |F_c||/\sum|F_o|$, for 6407 observed reflections. [b] $wR(F^2) = (\sum[w(F_o^2 - F_c^2)^2]/\sum[w(F_o^2)^2])^{1/2}$. [c] $S = [\sum[w(F_o^2 - F_c^2)^2]/(n - p)]^{1/2}$; n = number of reflections, p = number of parameters.

atoms, except those atoms of the $CNBu^t$ ligands and the triflate anion involved in disorder. All of the *tert*-butyl groups were found disordered in two positions, but five of them with a unique tertiary carbon, and were refined with geometrical restraints and a variable common carbon−carbon distance. The occupancy factors were refined but fixed complementary to 1.0 (C(9)−C(11) 0.63(3); C(13)−C(16) 0.57(1); C(19)−C(21) 0.55(4); C(23)−C(26) 0.71(2); C(35)−C(37) 0.54(2); C(39)−C(42) 0.62(2); C(45)−C(47) 0.52(2); C(50)−C(52) 0.61(1)). Hydrogen atoms of the nondisordered ligands (pyrazolate anions) were calculated and refined as riding on carbon atoms with a common isotropic displacement parameter. The function minimized was $\sum[w(F_o^2 - F_c^2)^2]$. The refinement converged to $R(F) = 0.0476$ ($F^2 > 2\sigma(F^2)$, 6407 reflections) and w$R(F^2) = 0.1421$ (all data) for 671 parameters, 170 restraints, and 10 940 unique reflections. The calculated weighting scheme was $1/[\sigma^2(F_o^2) + (0.0717P)^2]$, where $P = (F_o^2 + 2F_c^2)/3$. Scattering factors were used as implemented in the refinement program.[47]

Acknowledgment. We thank Dirección General de Investigación Científica y Técnica (DGICYT) for financial support (Project Nos. PB95-221-C1 and PB94-1186).

Appendix

Calculations of the extended Hückel type[48] were carried out using a modified version of the Wolfsberg−Helmholz formula.[49] The investigated compounds were modeled with internal symmetry using the geometrical parameters obtained from the reported crystal structure. Calculations and drawings were made with the program CACAO,[50] and the atomic parameters used are those implemented in this program.

Supporting Information Available: Tables of crystallographic data, atomic coordinates, isotropic and anisotropic thermal parameters, bond distances and angles, and least-squares planes for [**8**]CF_3SO_3 and an ORTEP diagram of [**8**]$^+$ (17 pages). Ordering information is given on any current masthead page.

OM970347J

(48) Hoffmann, R. *J. Chem. Phys.* **1963**, *39*, 1397. Hoffmann, R.; Lipscomb, W. N. *Ibid.* **1962**, *36*, 2179; **1962**, *37*, 2872.
(49) Ammeter, J. H.; Bürgi, H. B.; Thibeault, J. C.; Hoffmann, R. *J. Am. Chem. Soc.* **1978**, *100*, 3686.
(50) Mealli, C.; Proserpio, D. M. *J. Chem. Educ.* **1990**, *67*, 399.